

Broadband Nearfield Beamforming Using a Radial Beampattern Transformation

Rodney A. Kennedy, *Member, IEEE*, Thushara D. Abhayapala, *Student Member, IEEE*, and Darren B. Ward

Abstract—This paper presents a new method of designing a beamformer having a desired nearfield broadband beampattern. The methodology uses the spherical harmonic solution to the wave equation to transform the desired nearfield beampattern to an equivalent farfield beampattern. A farfield beamformer is then designed for a transformed farfield beampattern that, if achieved, gives the desired nearfield pattern exactly. Salient features of the new method are as follows.

- i) The nearfield patterns can be achieved for all angles, not just the primary look direction.
- ii) There is no theoretical restriction on the bandwidth.
- iii) General array geometries may be used.

As an illustration, we apply the method to the problem of producing a practical array design that achieves a nearfield beampattern that is frequency invariant over an octave bandwidth, where at the lowest frequency, the array-source separation is three wavelengths.

Index Terms— Array processing, broadband beamforming, nearfield beamforming.

I. INTRODUCTION

THE MAJORITY of array literature deals with the case in which the source is assumed to be in the farfield of the array. That is, the source is assumed to be at an infinite distance from the array, and hence, the received waveform from a single point source is planar. This significantly simplifies the solution to the beamforming problem. The common rule of thumb for the approximate distance at which the farfield approximation begins to be valid is $r = 2L^2/\lambda$, where

- r distance from an arbitrary array origin;
- L largest array dimension;
- λ operating wavelength [1].

Manuscript received August 6, 1996; revised December 18, 1997. This work was supported in part by the Australian Research Council and the Cooperative Research Centre for Robust and Adaptive Systems at the Australian National University under the Australian Government's Cooperative Research Centres Program. The associate editor coordinating the review of this paper and approving it for publication was Prof. Michael D. Zoltowski.

R. A. Kennedy is with the Telecommunications Engineering Group, RSISE, Australian National University, Canberra, Australia.

T. D. Abhayapala was with the Arthur C. Clarke Centre for Modern Technologies, Katubedda, Moratuwa, Sri Lanka. He is now with the Telecommunications Engineering Group, RSISE, Australian National University, Canberra, Australia.

D. B. Ward was with the Department of Engineering, FEIT, Australian National University, Canberra, Australia. He is now with the Acoustics and Speech Research Department, Bell Laboratories, Lucent Technologies, Murray Hill, NJ 07974 USA.

Publisher Item Identifier S 1053-587X(98)05224-6.

However, for complicated beampatterns with either low side-lobes or deep nulls, a distance of $10L^2/\lambda$ or more may be required [2], [3]. In many practical situations, the source is well within this distance, and using the farfield assumption to design the beamformer results in severe degradation in the beampattern. Furthermore, when broadband operation of the beamformer is required, which is the subject of this paper, the problem becomes more acute: At low frequencies, the source may appear in the nearfield, whereas at high frequencies, the same source may appear in the farfield of the array. We assume that every sensor that makes up the broadband array is identical and has a flat frequency response over the bandwidth of interest.

In this paper, a new method of nearfield beamforming is proposed in which a desired arbitrary broadband beampattern in both frequency and angle may be produced. The design methodology relies on two key tools: i) a transformation, using spherical harmonic solutions to the wave equation, which takes a nearfield beampattern specification and maps it to an equivalent farfield beampattern specification for a given frequency; and ii) a broadband beamforming method to realize a general angle-versus-frequency *farfield* beampattern specification. These tools combine to solve the nearfield broadband beamforming problem. As a special case of this work, we provide a method for narrowband nearfield design superior to conventional approaches (reviewed in Section II).

The paper is organized as follows. Section II describes the nearfield beamforming problem and the conventional method of designing nearfield beamformers. The general radial beampattern transformation is developed in Section III. Section IV simplifies the transformation for the special case of a linear array and presents an example. The problem of designing a beamformer to realize a general farfield angle-versus-frequency beampattern specification is addressed in Section V. Section VI then applies the method to the problem of nearfield frequency-invariant beamforming (an example that captures the full generality of the design methodology).

II. NEARFIELD COMPENSATION

In this section, a *nearfield compensation* method for designing nearfield beamformers is outlined based on applying time delays to compensate for the differing propagation delays assuming spherical propagation (see [4], for example). Other nearfield design methods exist that are based on numerical optimization (e.g., [5], [6]).

To illustrate nearfield compensation, consider a narrowband linear array of N sensors with a complex weight on each sensor. The response of the array to a signal at a distance r and angle θ (measured relative to endfire) from the zeroth sensor is

$$b_N(r, \theta) = \sum_{n=0}^{N-1} w_n \frac{r}{d_n(r, \theta)} e^{j2\pi f c^{-1}(d_n(r, \theta) - r)} \quad (1)$$

where w_n is the complex weight on the n th sensor, f is the frequency of operation, c is the speed of wave propagation

$$d_n(r, \theta) = (r^2 + 2r(x_n - x_0) \cos \theta + (x_n - x_0)^2)^{1/2} \quad (2)$$

is the distance from the source to the n th element, and x_n is the location of the n th element.

Compare this with the response to a farfield source at an angle θ , i.e.,

$$b_F(\theta) = \sum_{n=0}^{N-1} w_n e^{j2\pi f c^{-1} x_n \cos \theta}. \quad (3)$$

The goal of nearfield compensation is to transform the nearfield response to the farfield, such that standard farfield techniques can be used to design the array weights. In contrast to our method in Section III, this goal is not realized exactly, and the method only provides first-order correction over a limited range of angles.

The compensated nearfield response is

$$b_C(r, \theta) = \sum_{n=0}^{N-1} w_n \psi_n \frac{r}{d_n(r, \theta)} e^{j2\pi f c^{-1}(d_n(r, \theta) - r)}$$

where

$$\psi_n = r^{-1} d_n(r, \phi) e^{j2\pi f c^{-1}(r - d_n(r, \phi) + x_n \cos \phi)}$$

is the n th compensation term. It is seen that the compensated nearfield response is identical to the farfield response only at $\theta = \phi$ and is approximately equal for angles close to ϕ . To design a nearfield beamformer with a desired response, the weights w_n are obtained using standard farfield design techniques. The resulting compensated nearfield response is then approximately equal to the designed farfield response, at least over a range of angles. This is illustrated in Fig. 1, which shows a desired Chebyshev 25-dB response and the corresponding compensated nearfield response at a radial distance of three wavelengths from the center of a seven-element array. The uncompensated nearfield response (farfield design assumption) is shown as well. Clearly, nearfield compensation provides a significant improvement over an uncompensated array, although the compensated response still does not accurately achieve the desired response over all angles.

Yet another nearfield compensation method has given in [7], where the curvature of the spherical wavefront was approximated by a quadratic surface over the array aperture. However, designs based on this quadratic compensation method tend only to achieve the desired nearfield beampattern over limited angles closer to broadside, and it also ignores the variation of the magnitude with distance and angle.

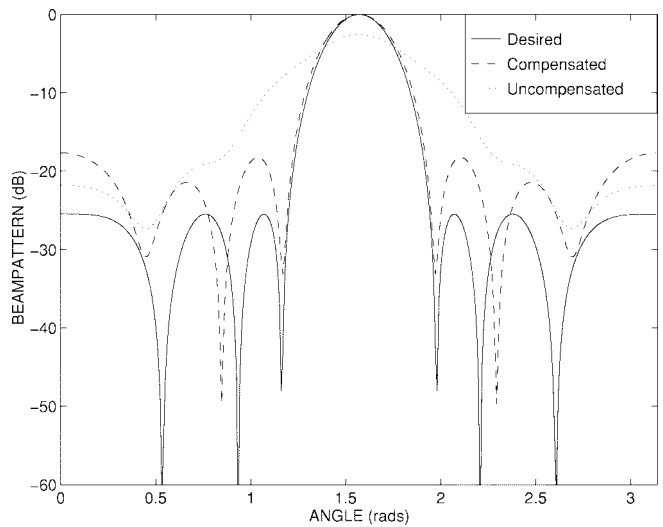


Fig. 1. Comparison of compensated and uncompensated nearfield beampatterns for a desired Chebyshev 25 dB beampattern at a radius of three wavelengths from the center of a seven-sensor array.

III. RADIAL TRANSFORMATION

A. Background

The nearfield compensation method is relatively straightforward to implement. However, the results achieved may fail to meet the desired design specifications (particularly in the sidelobes) since it only constrains the performance in a single direction (see Fig. 1). The nearfield beamforming method proposed here is to radially transform a nearfield pattern specification to a physically equivalent farfield pattern and design a farfield beamformer to realize this transformed farfield pattern. This equivalence, which we establish theoretically later in this section, means that we can obtain the desired nearfield response for all angles. We use the general solution to the wave equation to perform this radial transformation at a given frequency.

For a *broadband* nearfield beamformer, we would strictly want to perform this transformation over a continuum of frequencies. However, we can use the radial transformation developed for any particular frequency over a range of discrete frequencies to closely approximate this situation. Without loss of generality, we will develop the transformation using a spherical coordinate system, which is applicable to any three-dimensional (3-D) sensor array and any physically realizable beampattern. Since we express the nearfield beampattern specification on a sphere, which is a level surface of the spherical coordinate system, this is the natural coordinate system choice.

B. Wave Equation Solution

The transformation is obtained by solving the physical problem governed by the wave equation. Let r denote radial distance, and let ϕ and θ denote the azimuth and elevation angles, respectively, as shown in Fig. 2. Then, a general valid beampattern $b \equiv b(r, \theta, \phi, t)$ will satisfy the wave equation

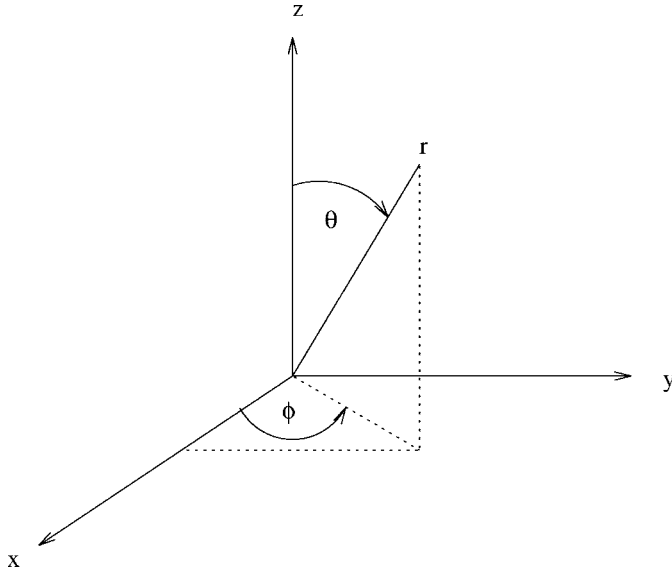


Fig. 2. Spherical coordinate system.

expressed in spherical coordinates

$$\begin{aligned} \frac{1}{r^2} \frac{\partial}{\partial r} \left(r^2 \frac{\partial b}{\partial r} \right) + \frac{1}{r^2 \sin \theta} \frac{\partial}{\partial \theta} \left(\sin \theta \frac{\partial b}{\partial \theta} \right) + \frac{1}{r^2 \sin^2 \theta} \frac{\partial^2 b}{\partial \phi^2} \\ = \frac{1}{c^2} \frac{\partial^2 b}{\partial t^2}. \end{aligned} \quad (4)$$

Conventionally, the time variation can be omitted as it clearly “separates” (as a variable) from the space variables. This leads to a conventional modulation at the frequency of interest.

The solution is classical [8], [9] and can be written (synthesis equation) as

$$\begin{aligned} b_r(\theta, \phi; k) = r^{-(1/2)} \left(\sum_{n=0}^{\infty} \alpha_n H_{n+1/2}^{(1)}(kr) P_n(\cos \theta) \right. \\ \left. + \sum_{n=1}^{\infty} \sum_{m=1}^n H_{n+1/2}^{(1)}(kr) P_n^m(\cos \theta) \right. \\ \left. \times (\beta_{nm} e^{jm\phi} + \gamma_{nm} e^{-jm\phi}) \right) \end{aligned} \quad (5)$$

where

$$k = \frac{2\pi f}{c}$$

is the wavenumber. The function $P_n(\cdot)$ is the Legendre function of order n ; $P_n^m(\cdot)$ are associated Legendre functions (which for $m = 0$ reduce to the Legendre functions). The radial dependency comes through a half integer order spherical Hankel function of the first kind, which is defined by

$$H_{n+1/2}^{(1)}(\cdot) = J_{n+1/2}(\cdot) + jY_{n+1/2}(\cdot)$$

where $J_{n+1/2}(\cdot)$ is a half integer order Bessel function of the first kind, and $Y_{n+1/2}(\cdot)$ is a half integer order Neumann function (or Bessel function of the second kind). Finally, we assume that the propagation speed c is independent of frequency, implying that k is a constant multiple of frequency

f . For this reason, throughout this paper, we will often refer to k as “frequency.”

The “choice” of the spherical Hankel function deserves some elaboration. The complete solution to the wave equation includes another term containing the spherical Hankel function of the second kind (complex conjugate of the spherical Hankel function of the first kind). By excluding this second term, we are excluding standing wave solutions, i.e., it is sufficient to consider either waves propagating generally away from the origin only or waves propagating generally toward the origin, but not both. The representation (5), therefore, is valid on a manifold (here, we choose a sphere) that encapsulates but does not penetrate the array.

With regard to analysis equations, the coefficients, assuming the beampattern specification is given on a sphere of radius r , are given by

$$\begin{aligned} \alpha_n = \frac{n + \frac{1}{2}}{2\pi r^{-(1/2)} H_{n+1/2}^{(1)}(kr)} \\ \times \int_0^{2\pi} \int_0^{\pi} b_r(\theta, \phi; k) P_n(\cos \theta) \sin \theta d\theta d\phi \end{aligned} \quad (6)$$

$$\begin{aligned} \beta_{nm} = \frac{n + \frac{1}{2}}{2\pi r^{-(1/2)} H_{n+1/2}^{(1)}(kr)} \frac{(n-m)!}{(n+m)!} \\ \times \int_0^{2\pi} \int_0^{\pi} b_r(\theta, \phi; k) P_n^m(\cos \theta) \sin \theta e^{-jm\phi} d\theta d\phi \end{aligned} \quad (7)$$

and

$$\begin{aligned} \gamma_{nm} = \frac{n + \frac{1}{2}}{2\pi r^{-(1/2)} H_{n+1/2}^{(1)}(kr)} \frac{(n-m)!}{(n+m)!} \\ \times \int_0^{2\pi} \int_0^{\pi} b_r(\theta, \phi; k) P_n^m(\cos \theta) \sin \theta e^{jm\phi} d\theta d\phi. \end{aligned} \quad (8)$$

Since the coefficients in the expansion (5) completely characterize the beampattern at all distances, the beampattern can be reconstructed for sources at arbitrary points in space. Because of the choice of spherical coordinate system, taking a nearfield beampattern specified on a sphere and subsequently transforming to the farfield infinite sphere leads to some computational savings in the above representations.

C. Procedure

The utility of the radial beampattern transformation is as follows. Given a beampattern $b_{r_1}(\theta, \phi; k)$ measured at some radius r_1 , calculate α_n , β_{nm} , and γ_{nm} from (6)–(8) with $r = r_1$. The beampattern can now be reconstructed for a source at any radius r_2 by using (5) with $r = r_2$.

The method we propose to design a nearfield beamformer is outlined below.

- 1) Calculate the beampattern coefficients for the desired nearfield beampattern $b_{r_d}(\theta, \phi; k)$ using (6)–(8) with $r = r_d$.
- 2) Calculate $b_{\infty}(\theta, \phi; k)$ from (5) at $r = \infty$.

- 3) Design a farfield beamformer to realize this beampattern using classical farfield array design techniques.

A curious feature of this formulation is that the actual array geometry is only of secondary importance. Any array geometry that can realize the resulting transformed farfield pattern may be used. This is important in a practical situation in which the array is mounted on a complex 3-D manifold, such as a microphone array mounted on the curved dashboard of a car. The question of whether a specific array can realize a specific farfield beampattern is a separate issue and is not addressed in this paper.

D. Nearfield Farfield Equivalence

Since the solution to the wave equation (4) is unique, there is an equivalent farfield beampattern for every nearfield beampattern specification and vice versa. Hence, using the farfield beamformer (which has been obtained in step 3 of Section III-C) in the nearfield at $r = r_d$ will produce the desired nearfield beampattern $b_{r_d}(\theta, \phi; k)$. To see this formally, observe that the coefficients in (6)–(8) are uniquely and completely determined once the beampattern is specified.

E. Farfield Normalization

The requirement to transform to $r = \infty$ exposes some potential numerical problems, which are resolved as follows. The half integer order spherical Hankel function of the first kind satisfies the asymptotic form [9]

$$\begin{aligned} H_{n+1/2}^{(1)}(kr) &\sim \sqrt{\frac{2}{\pi kr}} e^{j(kr - \pi(n+1)/2)} \\ &= (-j)^{n+1} \sqrt{\frac{2}{\pi kr}} e^{jkr} \quad \text{as } r \rightarrow \infty. \end{aligned}$$

Hence, in the synthesis equation (5), there is an attenuation with distance like r^{-1} , i.e.,

$$|r^{-1/2} H_{n+1/2}^{(1)}(kr)| \sim r^{-1}, \quad \text{as } r \rightarrow \infty.$$

Synthesis at $r = \infty$ gives $b_\infty(\theta, \phi; k) = 0$, which is clearly unacceptable. This can be easily compensated for by normalizing the magnitude of $b_r(\theta, \phi; k)$ by multiplying by r (this works because all modes exhibit this attenuation, i.e., it is independent of m and n).

The other problem is what phase to associate with $r = \infty$. This is somewhat arbitrary but is easily dealt with by setting the phase of the asymptotic half integer order spherical Hankel function to zero at a nominal frequency k_0 . For a narrowband design, k_0 would be simply the frequency of operation. For a broadband design, k_0 would typically be the midband frequency.

We thus obtain the farfield synthesis equation

$$\begin{aligned} \tilde{b}_\infty(\theta, \phi; k) &\sim \sqrt{\frac{2}{\pi k}} e^{j(k-k_0)} \left(\sum_{n=0}^{\infty} \alpha_n (-j)^{n+1} P_n(\cos \theta) + \sum_{n=1}^{\infty} \sum_{m=1}^n \right. \\ &\quad \left. \times (-j)^{n+1} P_n^m(\cos \theta) (\beta_{nm} e^{jm\phi} + \gamma_{nm} e^{-jm\phi}) \right) \quad (9) \end{aligned}$$

where \tilde{b} denotes a normalized beampattern.

IV. LINEAR ARRAY

A. Motivation for Special Case

The radial transformation developed in the previous section is sufficiently general to capture quite arbitrary three dimensional array geometries. In an attempt to bring the results into focus and provide a more concrete presentation of the ideas we examine a linear array aligned with the z axis. In this case the beampattern is rotationally symmetric with respect to ϕ , and the beampattern can be expressed as $b_r(\theta, \phi; k) = b_r(\theta; k)$.

B. Radial Transformation

The only nonzero components are those for which $m = 0$, which leads to the following simplified set of equations:

$$b_r(\theta; k) = \sum_{n=0}^{\infty} \alpha_n r^{-1/2} H_{n+1/2}^{(1)}(kr) P_n(\cos \theta) \quad (10)$$

and

$$\alpha_n = \frac{n + \frac{1}{2}}{r^{-(1/2)} H_{n+1/2}^{(1)}(kr)} \int_0^\pi b_r(\theta; k) P_n(\cos \theta) \sin \theta d\theta. \quad (11)$$

Applying the normalization described above we obtain the following farfield synthesis equation for a linear array aligned with the z axis.

$$\tilde{b}_\infty(\theta; k) \sim \sqrt{\frac{2}{\pi k}} e^{j(k-k_0)} \sum_{n=0}^{\infty} \alpha_n (-j)^{n+1} P_n(\cos \theta) \quad (12)$$

C. Parseval Relation

The synthesis equation (5) requires an infinite number of terms to exactly characterize the beampattern. In this section we derive a Parseval relation for the radial beampattern transformation and use it to provide an expression for the error in beampattern power associated with using a finite number of terms in the synthesis equation. Determining the number of modes to sufficiently accurately model the solution is an essential component of an efficient numerical procedure.

Rewrite (10) and (11) as

$$b_r(\theta; k) = \sum_{n=0}^{\infty} A_n P_n(\cos \theta) \quad (13)$$

and

$$A_n = (n + \frac{1}{2}) \int_0^\pi b_r(\theta; k) P_n(\cos \theta) \sin \theta d\theta \quad (14)$$

where $A_n = \alpha_n r^{-(1/2)} H_{n+1/2}^{(1)}(kr)$. Although A_n is a function of r and k , we suppress this dependence to simplify notation.

The Parseval relationship is derived through an application of (13) as

$$\int_0^\pi |b_r(\theta; k)|^2 \sin \theta d\theta = \sum_{n=0}^{\infty} \frac{1}{n + \frac{1}{2}} |A_n|^2. \quad (15)$$

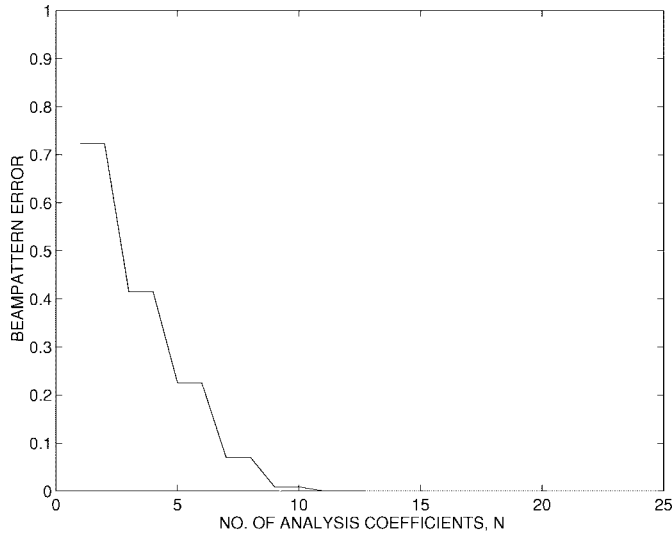


Fig. 3. Relative beampattern error versus the number of analysis coefficients calculated from (17) for a Chebyshev 25 dB beampattern at a radial distance of three wavelengths.

To approximate $b_r(\theta; k)$ by a finite series of the form

$$\hat{b}_r(\theta; k) = \sum_{n=0}^{N-1} \hat{A}_n P_n(\cos \theta) \quad (16)$$

we wish to find the \hat{A}_n that minimize the integral squared error between the desired beampattern $b_r(\theta; k)$ and the approximate beampattern $\hat{b}_r(\theta; k)$. As for the well-known case of a finite Fourier series representation, the minimum squared beampattern error is obtained by setting $\hat{A}_n = A_n$, for $n = 0, \dots, N - 1$, and the residual error is then given by

$$\begin{aligned} \epsilon &= \int_0^\pi |b_r(\theta; k) - \hat{b}_r(\theta; k)|^2 \sin \theta d\theta \\ &= \int_0^\pi |b_r(\theta; k)|^2 \sin \theta d\theta - \sum_{n=0}^{N-1} \frac{1}{n + \frac{1}{2}} |A_n|^2. \end{aligned} \quad (17)$$

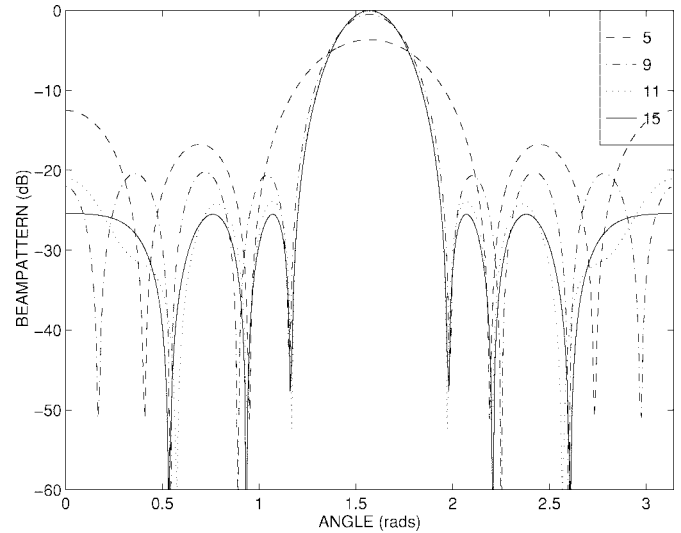
Thus, (17) gives the error associated with truncating the synthesis equation (10) to a finite number of terms.

D. Example

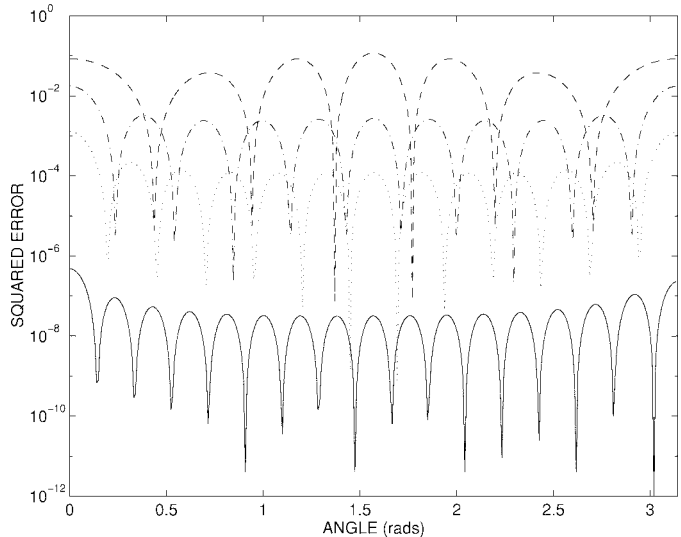
To illustrate the radial beampattern transformation, we revisit our previous example. The design was for a Chebyshev 25-dB beampattern (the desired beampattern in Fig. 1) at a radius of $r = 3$ wavelengths.

The relative beampattern error versus the number of analysis coefficients is shown in Fig. 3, calculated from (17). It is clear from this plot that at least ten analysis coefficients are required to provide a good approximation to the desired beampattern, and 15 coefficients capture essentially all the energy. The monotonically decreasing property displayed in Fig. 3 follows directly from (17).

To verify this, we calculated a set of 15 analysis coefficients from (11) at a radius of three wavelengths and then reconstructed the nearfield beampattern from (10) using different numbers of analysis coefficients. The resulting beampatterns are shown in Fig. 4, along with the squared error between



(a)



(b)

Fig. 4. Reconstructed beampatterns using different numbers of analysis coefficients for a desired Chebyshev 25-dB beampattern at a radial distance of three wavelengths. (a) Reconstructed beampatterns. (b) Squared beampattern error.

the desired and reconstructed beampatterns. With 15 coefficients, the reconstructed beampattern is indistinguishable from the desired Chebyshev 25-dB beampattern, and the squared beampattern error is uniformly less than 10^{-6} .

Using the set of 15 coefficients, we transformed the desired nearfield beampattern to the farfield using (12). We then designed a farfield beamformer to achieve this beampattern using a complex-valued least squares design criterion [10]. The least squares design equations are outlined in Section V-B.

The resulting beampattern realization for a symmetric linear array with 13 quarter wavelength spaced sensors is shown solid in Fig. 5. (Note that a quarter-wavelength spaced array was used since we found that it provided a better approximation to the farfield beampattern than a half-wavelength spaced array.) This farfield beamformer was then used in the nearfield at a radial distance of $r = 3$ wavelengths. The corresponding

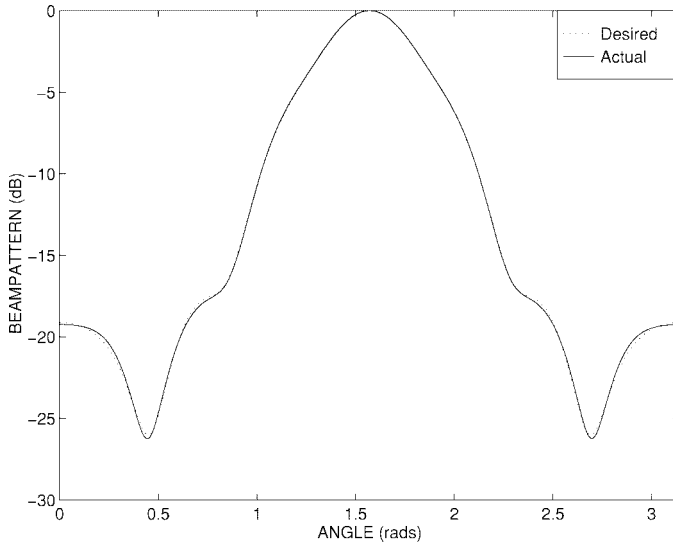


Fig. 5. Transformed farfield beampattern corresponding to a desired Chebyshev 25-dB beampattern at $r = 3$ wavelengths (dotted) and realization using an array of 13 quarter-wavelength spaced sensors (solid).

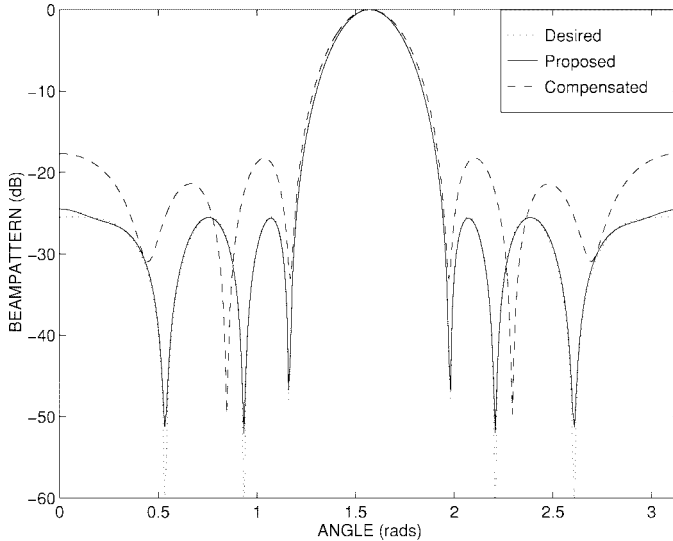


Fig. 6. Resulting nearfield beampattern (solid) from the proposed nearfield beamforming design technique for a desired Chebyshev 25-dB beampattern (dotted) at a radius of three wavelengths. The beampattern of a beamformer designed using nearfield compensation is also shown (dashed) for comparison.

beampattern is shown solid in Fig. 6, along with the desired nearfield beampattern, which is shown dotted. The proposed nearfield beamforming method provides a very close realization of the desired beampattern over all angles and not just at angles close to broadside as for the nearfield compensation method.

V. GENERAL BROADBAND BEAMFORMING

A. Background

Thus far, we have only considered application of the radial transformation at a single frequency. For a broadband nearfield beamformer, we would apply the radial transformation over a range of frequencies. Assuming radial symmetry in the ϕ

variable (i.e., for a linear array aligned with the z axis), this would produce a general farfield beampattern $b_\infty(\theta; k)$ specified over both angle θ and frequency k . In this section, we consider how to produce a farfield beamformer that realizes a general desired broadband beampattern.

For a broadband beamformer with a linear N sensor array, the response to plane waves arriving from an angle $u = \cos \theta$ with wavenumber (frequency) k is

$$a(u, k) = \sum_{n=0}^{N-1} H_n(k) e^{jkx_n u} \quad (18)$$

where x_n is the location of the n th sensor, and $H_n(k)$ is the frequency response of the filter on the n th sensor.

The problem we consider is to find the filter to apply to each sensor to achieve the desired general broadband beampattern. We refer to this as the *general broadband beamformer* (GOB) problem. We will outline some existing approaches to this problem and then propose a new solution.

B. Least Squares Design

The most straightforward, although not very illuminating, method of designing a GOB is through a least squares design criterion. Let the frequency response of the n th sensor filter be given by

$$H_n(k) = \sum_{m=0}^{M-1} h_n[m] e^{-jk c T m}$$

where

- $h_n[m]$ m th coefficient of the n th filter;
- c wave propagation speed;
- T sampling period.

The response of the GOB (18) may then be written in vector form as

$$a(u, k) = \mathbf{h}^H \mathbf{d}(u, k)$$

where \mathbf{h} is the vector of filter coefficients, and

$$\mathbf{d}(u, k) = [1, e^{-jk c T}, \dots, e^{-jk c T(M-1)}]^T \otimes [e^{jk x_0 u}, \dots, e^{jk x_{N-1} u}]^T$$

where \otimes denotes the Kronecker product.

Let $a_d(u, k)$ be a desired broadband response. If it is sampled at $P > NM$ points in angle-frequency space, then we obtain the following well-known overdetermined least squares problem [10]

$$\min_{\mathbf{h}} |\mathbf{D}^H \mathbf{h} - \mathbf{a}_d|^2$$

where $\mathbf{D} = [\mathbf{d}(u_1, k_1), \dots, \mathbf{d}(u_P, k_P)]$, and $\mathbf{a}_d = [\mathbf{a}(u_1, k_1), \dots, \mathbf{a}(u_P, k_P)]$. The solution to this problem is

$$\mathbf{h} = \mathbf{D}^\dagger \mathbf{a}_d$$

where $\mathbf{D}^\dagger = [\mathbf{D}^H \mathbf{D}]^{-1} \mathbf{D}^H$ is the pseudo-inverse of \mathbf{D} .

C. Discrete Fourier Transform Design

Alternative methods of designing a GOB are based on using the discrete Fourier transform. For a uniformly spaced array with the n th sensor located at $x_n = nd$ (where d is the intersensor spacing), the GOB response (18) may be expressed as a Fourier transform

$$a(u, k) = \sum_{n=0}^{N-1} H_n(k) e^{-j\omega n}$$

where $\omega = -k du$. Hence, if we sample the desired response at N points in u space, we obtain the discrete Fourier transform relationship

$$a(u_p, k) = \sum_{n=0}^{N-1} H_n(k) e^{-j2\pi pn/N} \quad (19)$$

for $p = 0, \dots, N-1$, and

$$H_n(k) = \frac{1}{N} \sum_{p=0}^{N-1} a(u_p, k) e^{j2\pi pn/N} \quad (20)$$

for $n = 0, \dots, N-1$.

For each frequency, the set of points at which the desired response is specified is

$$u_p = -\frac{2\pi p}{k d N}, \quad p = 0, \dots, N-1.$$

The sensor weights at this frequency are then given by the inverse discrete Fourier transform of the sampled desired response. This can be done for any number of frequencies within the design band. The coefficients for each sensor filter can then be found by conventional sampled frequency filter design techniques [11]. This approach has been recently used for the special case of designing a farfield beamformer that has a frequency invariant response over a wide bandwidth [12].

By carefully choosing the frequencies at which the desired response is sampled, it is possible to express the GOB response as a two-dimensional (2-D) discrete Fourier transform of the sensor filter coefficients [13]. In this case, the relationship is

$$a(u_p, k_q) = \sum_{n=0}^{N-1} \sum_{m=0}^{M-1} h_n[m] e^{-j2\pi pn/N} e^{-j2\pi qm/M} \quad (21)$$

where

$$h_n[m] = \frac{1}{NM} \sum_{p=0}^{N-1} \sum_{q=0}^{M-1} a(u_p, k_q) e^{-j2\pi pn/N} e^{-j2\pi qm/M}$$

is the m th coefficient of the n th sensor filter

$$u_p = -\frac{2\pi p}{k_q d N}, \quad p = 0, \dots, N-1$$

and

$$k_q = \frac{2\pi q}{M c T}, \quad q = 0, \dots, M-1.$$

D. New Design

The least squares design technique is a simple procedure, but it provides no insight into the underlying structure of the GOB problem. On the other hand, the Fourier transform methods are restricted to a uniformly spaced array geometry, whereas a nonuniform array geometry is more efficient in terms of number of sensors for broadband applications (see [14] for details). In this section, we propose a new method for the design of a GOB, which provides physical insight and allows a nonuniformly spaced array geometry.

Initially, consider a linear continuous aperture (rather than an array). The response of this aperture to planar waves arriving from an angle $u = \cos \theta$ (where θ is measured relative to endfire) is

$$a(u, k) = \int_{-\infty}^{\infty} \rho(x, k) e^{jkxu} dx \quad (22)$$

where $\rho(x, k)$ is the broadband aperture illumination or the response of the aperture at a point x and for a frequency k . This can be interpreted as a filter response (function of frequency k) at a displacement x (relative to some origin). For a finite aperture size, $\rho(x, k)$ will have finite support in x .

Temporarily fix the frequency to some arbitrary value $k = k_0$ and introduce $a_0(uk_0) = a(u, k_0)$, $\rho_0(x) = \rho(x, k_0)$, and $y = uk_0$. Substituting into (22) gives

$$a_0(y) = \int_{-\infty}^{\infty} \rho_0(x) e^{jyx} dx.$$

Thus, $a_0(y)$ is the inverse Fourier transform of $\rho_0(x)$, and

$$\rho_0(x) = \frac{1}{2\pi} \int_{-\infty}^{\infty} a_0(y) e^{-jyx} dy.$$

In general, the above relation holds for all values of k_0 . We thus have

$$a(u, k) = \int_{-\infty}^{\infty} \rho(x, k) e^{jkxu} dx \quad (23)$$

$$\rho(x, k) = \frac{k}{2\pi} \int_{-\infty}^{\infty} a(u, k) e^{-jkxu} du. \quad (24)$$

Thus, given a desired GOB response $a(u, k)$, the required aperture response at any frequency can be found through (24). Equation (23) represents the continuous aperture equivalent of (19).

Obviously, the continuous aperture required by (23) is not practical for beamforming with a finite number of point sensors. However, the problem of obtaining a desired GOB response using a discrete set of sensor locations reduces to the problem of approximating the integral in (23) by a summation of the form

$$\hat{a}(u, k) = \sum_{n=0}^{N-1} w_n(k) e^{jkx_n u}$$

where $w_n(k)$ is the complex weight on the n th sensor at a frequency k , i.e., a filter. We follow the approach introduced in [14], i.e.,

$$\hat{a}(u, k) = \eta \sum_{n=0}^{N-1} g_n \rho(x_n, k) e^{jkx_n u} \quad (25)$$

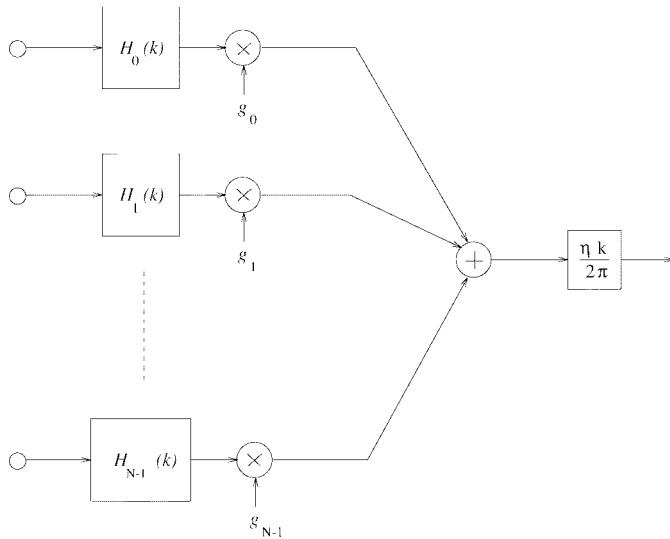


Fig. 7. Block diagram of the proposed general broadband beamformer.

where $\{x_n\}_{n=0}^{N-1}$ is a set of N discrete sensor locations; $\rho(x_n, k)$ is given by (24), where $a(u, k)$ is the desired GOB response; g_n is a *spatial weighting term*, which is used to account for the (possibly) nonuniformly spaced sensor locations; and η is a normalization constant (usually chosen such that $a(u_0, k_0) = 1$ for some angle u_0 and frequency k_0). See [14] for a full description of the spatial weighting terms and the choice of sensor locations.

Let the filter response on the n th sensor be

$$\begin{aligned} H_n(k) &= \frac{2\pi}{k} \rho(x_n, k) \\ &= \int_{-\infty}^{\infty} a(u, k) e^{-jkx_n u} du. \end{aligned} \quad (26)$$

We can therefore rewrite (25) as

$$\hat{a}(u, k) = \frac{\eta k}{2\pi} \sum_{n=0}^{N-1} g_n H_n(k) e^{jkx_n u} \quad (27)$$

and are thus led to the block diagram shown in Fig. 7. In this diagram, we have chosen to implement the common $k/(2\pi)$ term as a *secondary filter* to simplify the design of the individual *primary filters* $H_n(k)$. Note that the secondary filter may be perturbed slightly from its ideal differentiator form to normalize any scaling errors introduced by the approximation of (23) by the summation (27).

The utility of our proposed GOB technique is as follows. Given a desired angle-versus-frequency beampattern specification, calculate the filter responses from (26) at a number of frequencies. The primary filter coefficients may be then found by conventional frequency sampled filter design techniques [11]. Using these filters, the GOB is then implemented using the block diagram shown in Fig. 7.

The proposed GOB method represents a generalization of the previously presented farfield *frequency invariant beamformer* theory [14].

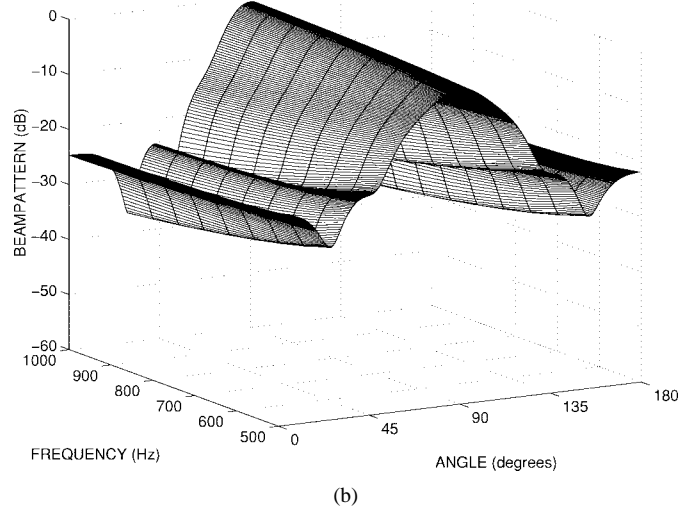
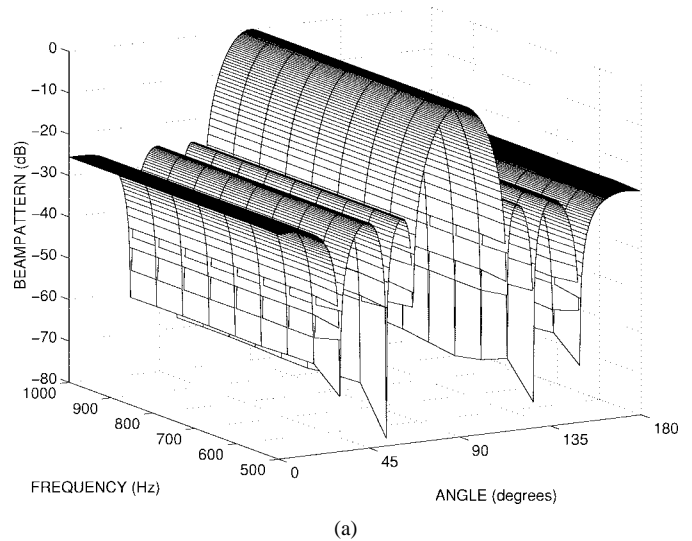


Fig. 8. Nearfield frequency invariant beampattern transformed from a radial distance of $3\lambda_L$ to the farfield. The beampattern is plotted at nine frequencies uniformly distributed within the range 500–1000 Hz. (a) Nearfield. (b) Farfield.

E. Application to Nearfield Beamforming

This GOB formulation can now be directly applied to the problem of implementing the transformed farfield broadband beampattern. Specifically, if $\tilde{b}_\infty(\theta; k)$ is the normalized broadband farfield beampattern resulting from a radial transformation of some desired broadband nearfield beampattern by (11) and (12), then the implementation equations are

$$\hat{b}_\infty(\theta; k) = \frac{\eta k}{2\pi} \sum_{n=0}^{N-1} g_n H_n(k) e^{jkx_n \cos \theta} \quad (28)$$

where

$$H_n(k) = \int_{-(\pi/2)}^{\pi/2} \tilde{b}_\infty(\theta; k) e^{-jkx_n \cos \theta} \sin \theta d\theta. \quad (29)$$

VI. NEARFIELD FREQUENCY INVARIANT BEAMFORMING

We now consider an example of the broadband nearfield beamforming technique outlined in this paper. Specifically,

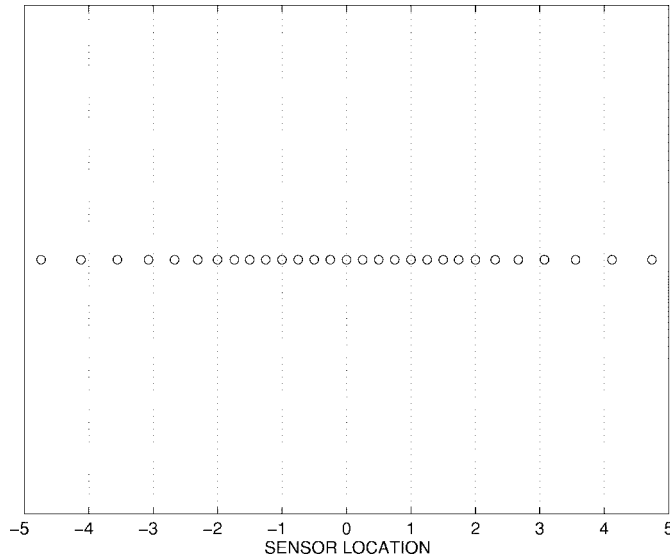


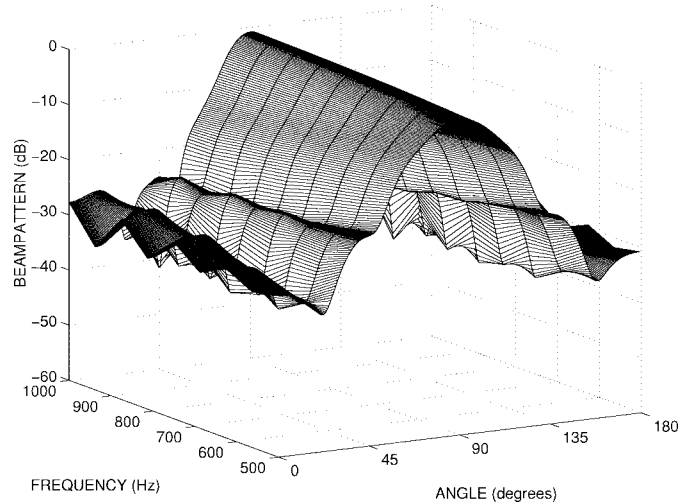
Fig. 9. Sensor locations used for the beamformer realization shown in Fig. 10. The locations are expressed in terms of λ_U , which is the wavelength corresponding to the upper frequency of operation.

we consider the design of a beamformer having a *frequency invariant* response in the nearfield, i.e., the nearfield response remains constant over a wide bandwidth. This design actually captures the full generality of the methodology since, in general, a nearfield frequency invariant beampattern transforms to a farfield frequency dependent beampattern, i.e., $b_r(\theta, \phi) \rightarrow b_\infty(\theta, \phi; k)$, $k \in [k_L, k_U]$, where $[k_L, k_U]$ is the bandwidth over which the nearfield beampattern is to be frequency invariant. This highlights the need for the general broadband beamforming theory developed in the previous section.

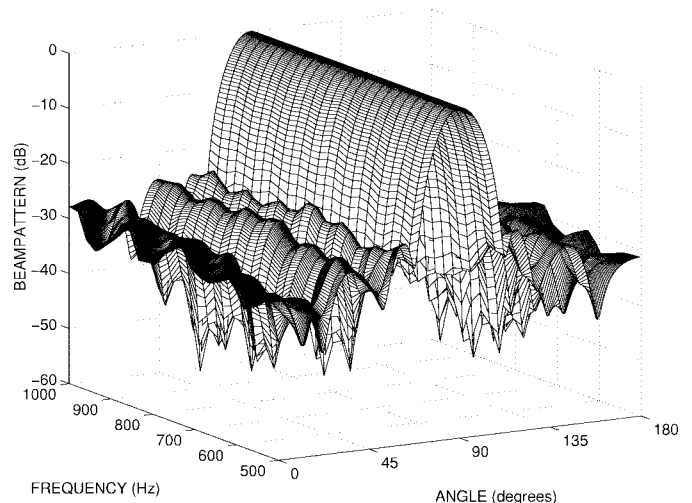
The design is for a nearfield beamformer having a Chebyshev 25-dB beampattern (shown as the desired beampattern in Fig. 1) over the frequency range 500–1000 Hz at a radial distance of $3\lambda_L$ (where λ_L is the wavelength corresponding to the lower design frequency $f_L = 500$ Hz). Note that at the upper design frequency ($f_U = 1000$ Hz), this corresponds to a radial distance of six wavelengths.

Using (11), a set of 25 analysis coefficients for the desired Chebyshev frequency invariant beampattern was calculated at a radius of $3\lambda_L$ for 9 frequencies uniformly distributed in the band. We note from Fig. 3 that 25 analysis coefficients are sufficient to produce negligible beampattern error. Applying (12), the farfield beampatterns were reconstructed for each of the nine design frequencies, resulting in the farfield beampatterns shown in Fig. 8. Hence, we see that the frequency-invariant nearfield beampattern is transformed to a frequency dependent farfield beampattern.

We then designed a general farfield beamformer of the structure shown in Fig. 7, with 32 complex coefficients for each sensor filter, to realize the farfield patterns shown in Fig. 8(b). The array consisted of 29 nonuniformly spaced sensors, located as shown by Fig. 9. Fig. 10(a) shows the realization of the desired farfield beampatterns shown in Fig. 8(b). This farfield beamformer was then simulated in the nearfield at a radial distance of $3\lambda_L$, and the resulting beampattern



(a)



(b)

Fig. 10. General farfield broadband beamformer designed to give the farfield beampatterns shown in Fig. 8(b). The farfield beampattern is shown at the nine design frequencies. The nearfield beampattern at a radial distance of $3\lambda_L$ is shown at the nine design frequencies plus 16 intermediate frequencies. (a) Farfield. (b) Nearfield.

is shown in Fig. 10(b). (The secondary filter was slightly perturbed from its ideal differentiator form to normalize slight scaling errors introduced by the implementation, as outlined in Section V.) Comparing this with the desired nearfield response of Fig. 8(a), we note that the desired nearfield frequency invariant response has been approximately achieved. The nearfield beampattern realization is also shown in Fig. 11, in which the beampatterns at 25 frequencies within the design band have been superimposed.

VII. CONCLUSIONS

A new method of broadband nearfield beamforming has been proposed in this paper. The methodology can be partitioned into two steps.

- 1) a wave-equation based technique to radially transform an arbitrary nearfield beampattern to a corresponding

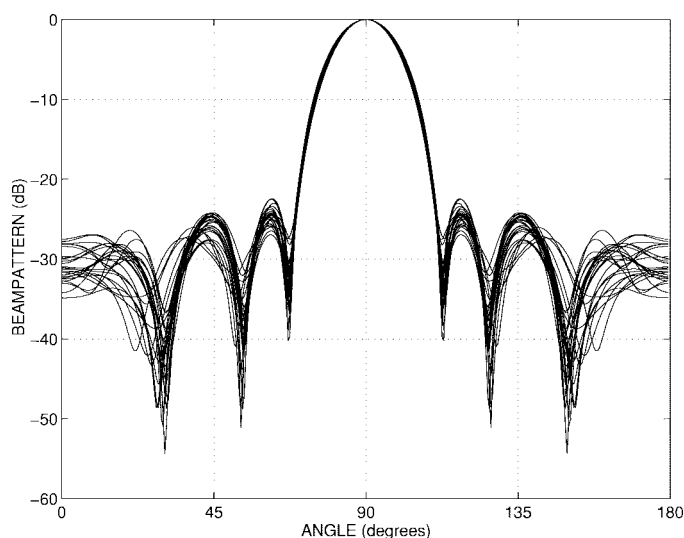


Fig. 11. Realization of a nearfield frequency invariant Chebyshev 25 dB beam pattern at a radial distance of $3\lambda_L$ over a frequency range of 500–1000 Hz. This figure is a superposition of the 25 beam patterns shown in Fig. 10(b).

farfield beam pattern (or beam pattern at any other radius);

- 2) a design method to achieve a desired farfield beamformer response specified over both angle and frequency.

REFERENCES

- [1] R. J. Mailloux, *Phased Array Antenna Handbook*. Boston: Artech House, 1994.
- [2] P. S. Hacker and H. E. Schrank, "Range distance requirements for measuring low and ultra low sidelobe antenna patterns," *IEEE Trans. Antennas Propagat.*, vol. AP-30, pp. 956–965, Sept. 1982.
- [3] R. C. Hansen, "Measurement distance effects on low sidelobe patterns," *IEEE Trans. Antennas Propagat.*, vol. AP-32, pp. 591–594, June 1984.
- [4] F. Khalil, J. P. Jullien, and A. Gilloire, "Microphone array for sound pickup in teleconference systems," *J. Audio Eng. Soc.*, vol. 42, pp. 691–700, Sept. 1994.
- [5] M. F. Berger and H. F. Silverman, "Microphone array optimization by stochastic region contraction," *IEEE Trans. Signal Processing*, vol. 39, pp. 2377–2386, Nov. 1991.
- [6] S. Nordebo, I. Claesson, and S. Nordholm, "Weighted Chebyshev approximation for the design of broadband beamformers using quadratic programming," *IEEE Signal Processing Lett.* vol. 1, pp. 103–105, July 1994.
- [7] B. D. Steinberg, *Principles of Array System Design: Including Random and Adaptive Arrays*. New York: Wiley, 1976.
- [8] C. A. Coulson and A. Jeffrey, *Waves: A Mathematical Approach to the Common Types of Wave Motion*. London, U.K.: Longman, 1977.
- [9] G. R. Balcock and T. Bridgeman, *The Mathematical Theory of Wave Motion*. Chichester, U.K.: Ellis Horwood, 1981.
- [10] B. D. Van Veen and K. M. Buckley, "Beamforming: A versatile approach to spatial filtering," *IEEE Acoust., Speech, Signal Processing Mag.*, vol. 5, pp. 4–24, Apr. 1988.
- [11] T. W. Parks and C. S. Burrus, *Digital Filter Design*. New York: Wiley, 1987.
- [12] T. Chou, "Frequency-independent beamformer with low response error," in *Proc. IEEE Int. Conf. Acoust. Speech Signal Process. (ICASSP)*, Detroit, MI, May 1995, pp. 2995–2998.
- [13] S. Haykin and J. Kesler, "Relation between the radiation pattern of an array and the two-dimensional discrete Fourier transform," *IEEE Trans. Antennas Propagat.*, vol. AP-23, pp. 419–420, May 1975.
- [14] D. B. Ward, R. A. Kennedy, and R. C. Williamson, "Theory and design of broadband sensor arrays with frequency invariant far-field beam patterns," *J. Acoust. Soc. Amer.*, vol. 97, pp. 1023–1034, Feb. 1995.



Rodney A. Kennedy (M'90) was born in Sydney, Australia, on October 23, 1960. He received the B.E. (hons.) degree in electrical engineering from the University of New South Wales, Sydney, in 1982. He received the M.E. degree in digital control theory from the University of Newcastle, Australia, in 1986. He received the Ph.D. degree in telecommunications from the Department of Systems Engineering, Australian National University, Canberra, in 1988.

From 1983 to 1985, he was a research engineer at CSIRO Division of Radiophysics, Sydney. Since 1994, he has been Head of Department of the Telecommunication Engineering Group, Research School of Information Sciences and Engineering, Australian National University. His research interests are in the fields of digital communications and signal processing.

Dr. Kennedy is currently an Associate Editor for Data Communications for the IEEE TRANSACTIONS ON COMMUNICATIONS.



Thushara D. Abhayapala (S'96) was born in Colombo, Sri Lanka, on March 1, 1967. He received the B.E. (hons.) degree in interdisciplinary systems engineering from the Australian National University, Canberra, in 1994. He is currently pursuing the Ph.D. degree at the Telecommunication Engineering Group, Research School of Information Sciences and Engineering, Australian National University.

From 1995 to 1997, he was employed as a Research Engineer at the Arthur C. Clarke Centre for Modern Technologies, Katubedda, Moratuwa, Sri Lanka. His research interest are in the areas of array processing and multidimensional signal processing.



Darren B. Ward was born in Mareeba, Australia, on September 12, 1970. He received the B.E. (hons) degree in electronic engineering and the B.A.S. degree in computer science from the Queensland University of Technology, Brisbane, Australia, in 1992, and the Ph.D. degree from the Department of Engineering, Australian National University, Canberra, in 1996.

Since December 1996, he has been a Postdoctoral Member of Technical Staff in the Acoustics and Speech Research Department, Bell Laboratories, Murray Hill, NJ. His research interests include signal processing, digital communications, and electroacoustics.